Quartz overgrowth textures and fluid inclusion thermometry evidence for basin-scale sedimentary recycling: An example from the Mesozoic Barents Sea Basin

Beyene G. Haile[1,*], Lina H. Line[1], Tore G. Klausen[3,4], Snorre Olaussen[1,2], Christian H. Eide[3], Jens Jahren[1], and Helge Hellevang[1,2]

1Department of Geosciences, University of Oslo, P.O.BOX 1047, Blindern, NO0316 Oslo, Norway

2The University Centre in Svalbard (UNIS), P.O.BOX 156, 9171 Longyearbyen, Norway

3Department of Earth Science, University of Bergen, Allegaten 41, 5007 Bergen, Norway

4Present address: Petrolia NOCO, Espehaugen 32, 5285 Bergen, Norway

**Corresponding author: b.g. haile@geo.uio.no*

ACKNOWLEDGEMENTS

This study was performed as part of the ISBAR (Internal and external forcing factors on the source-to-sink infill dynamics of the Lower Mesozoic Greater Barents Sea Basin) project, grant number 267689. We acknowledge financial support by PETROMAKS 2 programme of the Research Council of Norway (NRC) for the work reported on here. We acknowledge Carita Augustsson and Howri Mansurberg for critical and constructive comments markedly improving an earlier version of the manuscript. We are most grateful to Associate Editor Nadine McQuarrie for essential editorial handling. We are very grateful to Jan Inge Faleide and Alvar Braathen, University of Oslo, for sharing their knowledge about the tectonics-linked foreland basin evolution. We thank Siri Simonsen for her help with the SEM-CL analyses. All data to support our conclusions are archived at University of Oslo database. The data are available from the corresponding author upon reasonable request. There is no conflict of interest between authors.

ABSTRACT

Sedimentary recycling has the potential to obscure source-to-sink relationships, provenance interpretations, burial history reconstructions and robust reservoir quality predictions in siliciclastic sedimentary basins. Here, we integrate petrographic and cathodoluminescence microtextures with fluid inclusion thermometry in quartz overgrowths to identify sedimentary recycling and to constrain the potential provenance candidate for recycled grains in Lower Mesozoic sandstone of the western Barents Sea basin. Four diagenetic imprints were recognized as proof of sediment recycling: i) microtextural surface properties of overgrowths, ii) the presence of overgrowths at sutured grain contacts, iii) reversed diagenetic sequences and iv) fluid inclusions within quartz overgrowths. The diagenetic imprints confirm delivery of recycled sediments across the western Barents Sea basin. Their widespread distribution across the basin suggest that the recycled grains were derived from a drainage basin with regional-scale sediment dispersal potential during the latest Triassic. Furthermore, the drainage basin must have contained sedimentary rocks. Prior to surface exposure, the precursor sedimentary basin was subjected to burial temperatures exceeding 130ºC, whereby syntaxial quartz overgrowths precipitated. This temperature indicates an uplift of around 3–4 km, which represents a significant tectonic event. Recycled quartz grains can provide insights on their provenance as they retain direct temperature records. The geothermal signatures and geographically widespread distribution of recycled quartz exclude spatially restricted intrabasinal highs and higher-temperature crystalline rocks as provenance candidates for the recycled grain portion. Our data support the contemporaneous Novaya Zemlya Fold and Thrust Belt as the most likely provenance candidate in the region. The integrated approach demonstrated herein can be used to constrain sediment recycling and partly eroded provenance

candidates in sedimentary basins of equivalent setting worldwide, particularly in quartz-rich strata susceptible to sediment supply from older uplifted sedimentary basins.

Key words: Sedimentary recycling, Barents Sea basin, inherited quartz overgrowth, fluid inclusion thermometry, diagenetic imprints, Novaya Zemlya

INTRODUCTION

Sedimentary recycling has long been acknowledged as a problem in sedimentary petrology and basin analysis studies because it is difficult to evaluate the presence and abundance of first-cycle detritus as opposed to recycled grains (Augustsson et al., 2011; Blatt, 1967; Johnsson, 1993; McLennan & Taylor, 1980; Najman, 2006). As sediment derived from one provenance is remobilized and mixed with sediment from other sources, diagnostic traits of their source terrain are obscured. Although challenges associated with sediment recycling and its consequences for source-to-sink analyses are well known (Andersen, Kristoffersen, & Elburg, 2016; Moecher, Kelly, Hietpas, & Samson, 2019), the resulting implications for diagenetic modelling of sedimentary basins are largely ignored.

Geochemical, geothermometrical and geochronological analyses of individual detrital grains such as zircon, apatite, monazite, tourmaline and rutile constitute some of the conventional techniques for extracting petrogenetic information from the sedimentary record (von Eynatten & Dunkl, 2012). Although sedimentary recycling may be assessed by integrating geochronological and geothermal methods (Campbell, Reiners, Allen, Nicolescu, & Upadhyay, 2005; Tyrrell, Leleu, Souders, Haughton, & Daly, 2009), detrital geochronology and/or thermometry alone cannot overcome the ambiguity associated with recycled sedimentary rocks if the detrital grains carry no permanent record of sedimentary or diagenetic processes (Andersen et al., 2016). Apatite, monazite, tourmaline and rutile may also form authigenic phases during burial diagenesis but the use of heavy minerals as indicators of sedimentary recycling is limited due to their specific growth conditions, fragile crystals and volumetric insignificance in siliciclastic sediment(s) (Bouch, Hole, Trewin, Chenery, & Morton, 2002; Henry & Dutrow, 1992; Meinhold, 2010; Moecher et al., 2019; Morton & Hurst, 1995). This poses a particular problem for quartz-rich sandstone, where quartz grains often constitute the sole means for unravelling the sediment history (Blatt, 1967).

In contrast to other methods used to evaluate sediment recycling, authigenic quartz overgrowth is volumetrically significant in sedimentary basins worldwide and can be used to identify sediment recycling in siliciclastic rocks (e.g., Sanderson, 1984). Syntaxial quartz overgrowths with euhedral crystal interfaces can form continuously by direct precipitation of silica from aqueous solutions at burial temperatures exceeding 70°C (Bjørlykke & Egeberg, 1993; Land & Fisher, 1987; Walderhaug, 1996; Worden & Morad, 2000). As quartz cement covers the surfaces or fracture walls of detrital quartz grains, microscopic pockets of diagenetic fluid may occasionally be trapped between the detrital grain and the cement (Bodnar, 2003a). These fluid inclusions tend to be chemically non-reactive and will only undergo reversible phase transitions upon later changes in temperature and pressure. Thus, a fundament for obtaining homogenization temperatures is established (Bodnar, 2003b; Goldstein, 2001; Roedder, 1984). Slow precipitation rates make the quartz cementation process insensitive to periods of increased heat flow (e.g., hydrothermally induced heat flow from magmatic activity) and overprinting by subsequent uplift episodes (Haile, Klausen, Jahren, Braathen, & Hellevang, 2018; Worden & Burley, 2003). As such, fluid inclusions carry permanent fingerprints of the temperature conditions at the time of entrapment and can therefore store geothermal records from former burial cycles (Bjørlykke & Egeberg, 1993; Hollister et al., 1981; Walderhaug, 1994).

Microtextural surface properties of quartz overgrowths represent the simplest and most commonly applied technique in identifying sediment recycling (Dott, 2003; Götte & Richter, 2006; Johnsson et al., 1988). Rounded quartz overgrowths are found from several stratigraphic intervals and geographic locations worldwide (Caja Rodríguez et al., 2008; Dott, 2003; Götte & Richter, 2006; Johnsson, Stallard, & Meade, 1988; Olaussen, Dalland, Gloppen, & Johannessen, 1984; Rezaee & Tingate, 1997; Ulmer-Scholle, Scholle, Schieber, & Raine, 2014; Walderhaug & Bjørkum, 2003) and diagenetic imprints in quartz are stable on geological timescales. This implies that single quartz grains have the potential to preserve several diagenetic imprints throughout the sedimentation processes. Petrographic and thermal properties of quartz overgrowths can therefore be used to constrain sedimentary recycling and provenance rock types in siliciclastic sediment(s) in modern and ancient sedimentary basins globally. The diagenetic imprint in quartz is also suitable for distinguishing *in situ* from inherited quartz overgrowth when estimating quartz cementation and ultimately assessing the reservoir quality of quartz-rich sandstones.

This study aims to: i) evaluate the combined use of petrography, cathodoluminescence and fluid inclusion thermometry for proving sedimentary recycling, and ii) demonstrate how the combined approach can exert constraints on provenance rock type and potential provenance source. Upper Triassic to Middle Jurassic strata from the Barents Sea basin (Fig. 1) were selected as a case study because the succession records a shift from a high- to low-accommodation basin architecture (Line, Müller, Klausen, Jahren, & Hellevang, 2020; Müller et al., 2019; Ryseth, 2014). Although the hinterland reconfiguration that occurred during the Triassic-Jurassic transition is thoroughly documented along the southern margin of this basin (Bergan & Knarud, 1993; Mørk, 1999; Ryseth, 2014), landscape development in the eastern provenance regions remain uncertain.

GEOLOGICAL SETTING

During the Triassic, the Barents Sea basin constituted an epicontinental seaway on the northern coast of the Pangea supercontinent (Golonka, 2007; Golonka, Embry, & Krobicki, 2018;

Worsley, 2008). The Barents Sea was characterized as a high-accommodation basin, where the sedimentary basin infill reached thicknesses up to several kilometres in some areas (Faleide et al., 2018; Müller et al., 2019). North-westerly prograding clinoforms sourced from the Uralide Orogen southeast of the Barents Sea dominated the basin infill and channel systems sourced from this hinterland terrain could be up to 20 km wide (Glørstad-Clark, Faleide, Lundschien, & Nystuen, 2010; Klausen, Ryseth, Helland-Hansen, Gawthorpe, & Laursen, 2014). Sediment supply from the Caledonian and Fennoscandian hinterlands in the south was limited and restricted to the southern margins of the basin throughout most of the Triassic (Klausen, Müller, Slama, & Helland-Hansen, 2017).

From the Late Triassic to Early Jurassic, the western Barents Sea transitioned from a high- to a low-accommodation basin (Ryseth, 2014). Rejuvenation of the Caledonian and Fennoscandian hinterlands resulted in a pronounced shift in depositional trends along the southern margins of the basin, where southerly-derived sediment largely replaced Uralide provenance signatures (Bergan & Knarud, 1993; Line, Reidar, Tore, Jens, & Helge, 2020; Ryseth, 2014). By contrast, petrographic and geochronological data from the basin interior indicate no pronounced change in provenance across the Carnian-Norian boundary, where mineral characteristics and zircon ages associated with the Uralide Orogeny prevail (Fleming et al., 2016; Line et al., 2020). Simultaneously, compressional tectonic forces in the east facilitated advancement of the Novaya Zemlya Fold-and-Thrust Belt and the associated forebulge development in the central Barents Sea basin (Faleide et al., 2018; Müller et al., 2019). The structural reconfiguration of the basin and the surrounding hinterland terrains brought about dramatic thickness variations and condensation of the Lower Mesozoic successions in the western Barents Sea (Olaussen et al., 2018; Worsley, 2008). The exact timing and driving mechanism of the compressional tectonic phase are presently poorly constrained (Pease, 2011; Toro, Miller, Prokopiev, Zhang, & Veselovskiy, 2016).

On Svalbard, the Upper Triassic to Middle Jurassic succession is collectively referred to as the Wilhelmøya Subgroup, which includes the Flatsalen, Svenskøya and Kongsøya formations (Mørk et al., 1999) (Fig. 1B). In general, the formations constitute mature sandstones deposited in deltaic to shallow marine environments (Mørk et al., 1999; Rismyhr, Bjærke, Olaussen, Mulrooney, & Senger, 2019). The Flatsalen Formation is composed of feldspathic litharenite and the Svenskøya Formation is characterized as sublitharenite to subfeldsarenite (Haile et al., 2019). The Flatsalen and Svenskøya formations contain very fine to medium-grained sediment, predominantly moderately well sorted. Minor early diagenetic alterations such as the formation of pore-filling kaolinite and minor mechanical plastic deformation of ductile grains are documented (Haile et al., 2019). Thin early calcite cemented intervals are recorded in the Flatsalen Formation. Across the northern Barents Sea basin, the upper part of the Wilhelmøya Subgroup, the Kongsøya Formation displays condensed sections with numerous hiatuses associated with limited accommodation space, sediment starvation, and erosion (Anell, Braathen, & Olaussen, 2014). Surface exposures on Wilhelmøya, Svalbard, display a section of poorly consolidated strata with burial temperature estimates in the range of 50 - 60°C (Haile et al., 2019; Mørk & Bjorøy, 1984).

The Upper Triassic to Middle Jurassic subsurface equivalent in the interior of the Barents Shelf is the Realgrunnen Subgroup, which comprises the Fruholmen, Tubåen, Nordmela and Stø formations (Worsley, Johansen, & Kristensen, 1988) (Fig. 1B). These formations were deposited in coastal plain and deltaic to shallow marine environments (Klausen, Müller, Poyatos-Moré, Olaussen, & Stueland, 2019; Lord, Mørk, Mørk, & Olaussen, 2019; Mulrooney et al., 2018; Mørk et al., 1999). The subgroup is thicker than its onshore counterpart but thin compared to underlying Triassic units. The Fruholmen Formation in the basin interior is characterized as sublitharenite, with the grain size ranging from coarse silt to fine-grained sand. Quartz, feldspar and argillaceous minerals constitute the framework minerals. In the sandy Stø Formation, fine- to medium-grained quartz make up the principal framework minerals (Line et al., 2020). The cement phases in the Fruholmen and Stø formations (wells 7124/3-1, 7220/7-2S, 7324/7-2, 7324/8-1 and 7324/9-1) are minor authigenic quartz cement (<2%), pore-filling kaolinite and carbonate cement. The *in situ* authigenic quartz cement indicate a minimum burial temperature of 70 - 80°C (Walderhaug, 1994) which is consistent with the estimated net exhumation trends (~1800 m) in the southwestern Barents Sea (Baig, Faleide, Jahren, & Mondol, 2016).

The Barents Sea region has been subjected to several episodes of major differential uplift and erosion since the Mesozoic (Anell, Thybo, & Artemieva, 2009; Baig et al., 2016; Henriksen, Ryseth, et al., 2011; Ohm, Karlsen, & Austin, 2008; Sobolev, 2012). The burial history indicates differential deposition and erosion during the Late Triassic-Middle for different areas of the Barents Sea basin (Klausen, Müller, Poyatos-Moré, Olaussen, & Stueland, 2019). During the Cenozoic, the magnitude of uplift increased northward to up to 2500 m in the northwestern Barents Sea (Nyland, Jensen, Skagen, Skarpnes, & Vorren, 1992) compared to the southwestern Barents Sea, which experienced 500–1800 m erosion (Baig et al., 2016; Henriksen, Bjørnseth, et al., 2011). Petrophysical well data indicate that the centre of the southeastern Barents Sea basin experienced the least exhumation (400 ‑ 500 m), whereas the uplift magnitude increased northward up to 2000 m in the northeastern Barents Sea (e.g. on Franz Josef Land) (Sobolev, 2012).

MATERIALS AND METHODS

Samples for this study were collected from unconsolidated outcrop units on Wilhelmøya and time equivalent sandstone strata in the interior of the western Barents Sea basin, situated approximately 610 km apart (Table 1, Fig. 1A–B). Analyses using transmitted light microscope microtexture/image features and scanning electron microscope imaging coupled with cathodoluminescence (SEM-CL) were performed on sixteen samples that together form a representative range of the recycled lithologies. SEM-CL micrographs were obtained using a Hitachi SU5000 FEG-SEM integrated with a Delmic SPARC high-performance SEM-CL detector at the Department of Geosciences, University of Oslo. Quartz overgrowths are clearly demarcated from detrital quartz grains by the luminosity contrast between dark quartz overgrowths and bright detrital quartz grains. The CL micrographs were acquired using an acceleration voltage of 12 kV and working distance of 13 mm. Red-green-blue (RGB) colour images were generated by combining three images by using red, green and blue filters. Data acquisition and fine-tuning of the RGB images were conducted using the Delmics odemis software. The cathodoluminescence RGB coupled with cathodoluminescence intensity imaging method was applied in order to differentiate between overgrowths of different generations.

Primary fluid inclusions at grain-overgrowth boundaries or within overgrowths were used to determine the crystallization temperature of the quartz overgrowths. Homogenization temperatures were measured from polished thick sections (~70 μm) at the China University of Petroleum, Qingdao, China, using a Zeiss Axioscope A1 APOL digital transmission microscope coupled with a calibrated Linkam TH-600 heating and cooling stage. Homogenization temperatures were determined using a heating rate of 10 °C/min at temperatures below 60 °C and 5 °C/min above 60 °C. The measured temperature precision for homogenization temperature is ±1 °C.

RESULTS

Quartz Overgrowth characteristics

Detrital quartz grains covered by syntaxial quartz overgrowths with abraded and rounded textures are observed through microscope and cathodoluminescence micrographs in all studied samples (Fig. 2A–B), inferring a widespread occurrence across the western Barents Sea basin.

Detrital quartz grains are distinguished from authigenic overgrowth by the presence of dust rims in plane polarized light (Fig. 2C).

A quantification estimate from the Svenskøya Formation from Wilhelmøya suggest that around 10-15% of the grain assembly contain abraded quartz overgrowths. Rounded overgrowths in quartz-rich sediment from the Flatsalen and Svenskøya formations yield fluid inclusion homogenization temperatures ranging from 90°C to 130°C (Fig. 2D). In addition, microcrystalline quartz coats were observed on the top of well-rounded and abraded quartz overgrowths that formed directly on detrital quartz grains (Fig. 3A-C). Euhedral quartz overgrowths were not observed in the host sediment on Wilhelmøya.

In the basin interior, approximately 20% of the grains have rounded overgrowth surface textures (Fig. 4A). Penetrating quartz overgrowths were observed at sutured intergranular contacts between two detrital quartz grains in a sandstone sample from the Upper Triassic Fruholmen Formation (Fig. 4B). In the overlying quartz arenitic Stø Formation, cathodoluminescence contrasts and RGB micrographs show two generations of quartz overgrowths (Fig. 4C-D). The inner zone of quartz cement that encloses the detrital quartz grain appears rounded, whereas the outer quartz overgrowth displays euhedral to subrounded surface textures. The inner quartz overgrowth shows alternating luminescent bands whereby the crystals grew parallel to the crystal faces of the detrital quartz grain (Fig. 4C). By contrast, the outer overgrowth displays uniform and dark luminescence with a homogeneous crystal growth pattern (Fig. 4C). By SEM-CL RGB imaging, the inner zone appears dark blue, whereas the outer zone has a dark brown appearance (Fig. 4D). No fluid inclusion homogenization temperatures are available from the Lower Mesozoic strata in the Basin interior.

DISCUSSION

Identifying sediment recycling from quartz overgrowth textures and fluid inclusion thermometry

The rounded edges signify that the overgrowths were exposed to weathering and/or abrasion at the surface at least once after it precipitated at depth (Fig. 5A) because syntaxial quartz cement forms euhedral crystal interfaces at 70°C (Bjørlykke & Egeberg, 1993). The high abundance of rounded and abraded quartz overgrowths in the Lower Mesozoic strata of the western Barents Sea basin may thus be regarded as compelling evidence for sediment recycling.

In addition to the rounded syntaxial overgrowths, the authigenic quartz cement at sutured grain contacts, microstylolites, can be used as a means to recognize sedimentary recycling (Fig. 5B). Pressure dissolution (stress) induces mutual interpenetration of detrital quartz grains, observable as microstylolites. At grain contact or microstylolite interfaces, silica dissolution is catalysed by the presence of clay minerals (Walderhaug & Bjørkum, 2003). Authigenic quartz overgrowths cannot form at sutured grain contacts because dissolved silica redistributes away from the contact interface and precipitates at grain surfaces adjacent to the point of contact (Oelkers, Bjørkum, Walderhaug, Nadeau, & Murphy, 2000). Precipitation of quartz cement occur first during onset of chemical compaction at 70ºC (Morad, Ketzer, & De Ros, 2000) as it is commonly considered that the main source of quartz cement in sedimentary basins is intergranular pressure dissolution along stylolites (Oelkers, Bjørkum, & Murphy, 1996; Walderhaug, 1996). Thus, the presence of authigenic quartz cement at microstylolite interfaces represents an inherited feature that formed prior to mechanical compaction and constitute compelling evidence for sediment recycling.

The reversed diagenetic sequence documented in the Svenskøya Formation from Wilhelmøya, with microcrystalline quartz covering rounded syntaxial overgrowths (Fig. 5C), is inconsistent with sequences expected in normal burial scenarios. At shallow depths (~ < 2 km) and in the presence of biogenic or other metastable silica solids, silica saturations may reach such high levels that microquartz nucleates and grows directly on detrital grains (Ramm, Forsberg, & Jahren, 1997). When sediment is buried to 2-3 km depth and temperatures reach about 70°C, larger crystals may form as syntaxial overgrowths on existing quartz grains (Bjørlykke & Egeberg, 1993; Walderhaug, 1994). The reversed diagenetic sequence cannot be accounted for by tectonic uplift because the major source of amorphous silica that produce high silica supersaturation to form microquartz derives mainly from biogenic detritus entering the system during the depositional sequence. Hence, the reverse diagenetic signature argues in favour of sediment recycling.

The observed multiple generations of quartz overgrowths is an additional sign of sediment recycling (e.g., Basu, Schieber, Patranabis-Deb, & Dhang, 2013). The inner quartz overgrowth with rounded surfaces observed in the Stø Formation likely represents an inherited cement phase, whereas the outer rim overgrowth with euhedral to subrounded surface texture represents a subsequent cement phase postdating final deposition. Inherited quartz overgrowths, particularly those enclosed by subsequent euhedral overgrowths (Fig. 5D), are easily overlooked and misinterpreted as *in situ* cement by optical microscope analysis alone unless dust rims are present (e.g., Cooper, Evans, Flint, Hogg, & Hunter, 2000;Austin, 1974; Basu et al., 2013; Burley, Mullis, & Matter, 1989). Regardless of whether dust rims are present or not, SEM RGB (coloured) CL imaging can be used to differentiate multiple quartz overgrowths from each other (e.g., Basu et al., 2013). The CL contrasts between the inner and outer overgrowths show a divergent microstructure possibly as consequence of changing physio-chemical conditions during their formation processes. Such type of growth zoning within quartz overgrowths could result from defects in the crystal lattice typically caused by incorporation of trace elements (e.g., Götte, 2018; Lehmann, Pettke, & Ramseyer, 2011). Blue and brown RGB CL luminescence for the inner and outer overgrowths, respectively, suggests differences in temperature at the time of quartz precipitation. Brownish luminescence overgrowth has been associated with lower temperature (80-100ºC) quartz cement whereas blue CL luminescence reflects higher temperature ranges (150-220ºC) (Richter, Götte, Götze, & Neuser, 2003). Higher-temperature overgrowths enclosed by lower-temperature overgrowths, as documented herein, represent a reversed diagenetic sequence incompatible with one continuous burial cycle. The combined use of petrography, SEM-CL intensity and RGB CL micrographs presented herein identifies inherited quartz overgrowths and suggest at least two phases of burial sequences the detrital grain was subjected to. To our knowledge, this combined approach is the first to differentiate multiple quartz overgrowth generations.

As quartz cementation occurs as a continuous process (Walderhaug, 1994), the homogenization temperatures documented from fluid inclusions within rounded quartz overgrowths from Wilhelmøya imply that the grains have been subjected to at least 130ºC.The thermal history of rounded quartz cement recorded herein deviates significantly from the burial history of the host sediment. The recorded homogenization temperatures are substantially higher than other temperature estimates for the northwestern Barents Shelf, which lie in the range of 50 - 60°C (Haile et al., 2019; Mørk & Bjorøy, 1984). Moreover, the studied succession on Wilhelmøya has recorded no diagenetic fingerprints that suggests temperatures exceeding 70–80 °C (Haile et al. 2019). This is supported by the absence of *in-situ* euhedral quartz overgrowths. The unconsolidated nature of the Lower Mesozoic succession on Wilhelmøya (Haile et al., 2019; Lord et al., 2019) further substantiates a shallow and low-temperature burial scenario of the host sediment (Olaussen et al., 2018). Unconsolidated grains carrying fluid inclusions with homogenization temperatures that deviate significantly from established burial and temperature trends of the host sediment may therefore be considered as extrabasinal and recycled. This study is the first to recognize fluid inclusion thermometry as evidence for sedimentary recycling.

Constraining provenance rock type from fluid inclusion microthermometry

The abraded quartz overgrowths with fluid inclusion temperatures of 130°C from the Lower Mesozoic strata on Wilhelmøya are indicative of a diagenetic origin and infers that the recycled grains are derived from a drainage basin where consolidated sedimentary rocks were exposed. This geothermal signature excludes crystalline rock types as potential provenance candidates for the recycled grain portion. The recorded temperatures indicate that the recycled grains reached a depth of 3-4 km during their precedent burial cycle assuming a paleo-geothermal gradient of 40°C/km for the Barents Shelf (Braathen et al., 2012). As a result, the sedimentary provenance rocks must have undergone substantial uplift (> 4 km) prior to surface exposure during the Latest Triassic.

Surface exposures of consolidated sedimentary rocks could occur at (i) locally uplifted parts of the Barents Sea, or (ii) within an extrabasinal hinterland where uplifted sedimentary strata constituted a part of the drainage basin. This implies that either of these two candidates must have been the source of the recycled grains. Apart from the present study area, abraded quartz overgrowths are also detected in Jurassic sandstone strata from other parts of the southwestern Barents Sea basin (Olaussen et al., 1984; Walderhaug & Bjørkum, 2003), attesting to a widespread occurrence of recycled components in the Late Triassic–Middle Jurassic sedimentary system of the Barents Sea basin. The high quantitative estimates and widespread distribution of abraded quartz overgrowths across the Barents Sea basin suggest the supply of recycled grains were significant, possibly reflecting a laterally extensive provenance area. Paleogeographic reconstructions, tectonic syntheses (Doré, 1991; Sømme, Doré, Lundin, & Tørudbakken, 2018; Ziegler, 1988) and structural models (Anell, Faleide, & Braathen, 2016; Faleide, Vågnes, & Gudlaugsson, 1993; Faleide et al., 2018) of the Barents Sea region does not record exposed paleo-highs during the Late Triassic. However, deep erosion has been documented over the Fedynsky High during the Late Triassic to Early Jurassic (Müller et al., 2019), although this confined intrabasinal high is not large enough to explain the widespread distribution of recycled grains in the basin during the latest Triassic. Consequently, intrabasinal highs in the Barents Sea are not considered as probable sources for the recycled detritus investigated herein.

An absence of quartz with recycled overgrowth in the underlying Early-Middle Triassic strata indicates different source areas and thus that the consolidated sedimentary provenance rock did not become a significant supplier of sediment to the Barents Sea basin until the latest Triassic (Norian) (Line et al., 2020). The recycled grains entered the basin shortly after a regional shift in fluvial channel architecture occurred in the western Barents Sea, which was interpreted as a basin response to the Late Triassic Novaya Zemlya phase of the Uralian Orogeny (Klausen et al., 2014). Moreover, apatite fission track data and thermal modelling using Palaeozoic sedimentary rocks indicate that rapid cooling occurred on Novaya Zemlya between 220 & 201 Ma (Zhang, Pease, Carter, & Scott, 2018) , suggesting the archipelago was uplifted during the Late Triassic (Faleide et al., 2018). As the closest tectonically active region at the time of sediment deposition, and with the entire Mesozoic succession missing (Drachev, 2016; Faleide et al., 2018; Klausen et al., 2017; Müller et al., 2019; Olaussen et al., 2018), uplifted and eroded strata on Novaya Zemlya represents the most credible provenance candidate for the recycled grain assembly in the studied successions.

A schematic representation of basin-scale sedimentary recycling in response to uplift in Novaya Zemlya is illustrated in Figure 6. During most of the Triassic, geochronological and mineralogical signatures in the grains indicate transport from the Uralide Orogen into and across the Greater Barents Sea basin (Bue & Andresen, 2014; Mørk et al., 1999; Klausen et al., 2017; Klausen et al., 2019). Positioned at the northern edge of the Polar Uralides, it is likely that the Novaya Zemlya area constituted a proximal part of the high-accommodation basin and therefore shares mineralogical and geochronological signatures with sediment derived from the Uralian Orogen (Fig. 6A). Exhumation and denudation of the basin strata may have remobilized grains with the Uralide signatures from the Novaya Zemlya area to the western Barents Sea basin (Fig. 6B) as the Novaya Zemlya Fold and Thrust Belt developed during the Latest Triassic (Faleide et al., 2018). Consequently, the only detectable difference between recycled Triassic grains from the uplifted Novaya Zemlya archipelago and other (possible first-cycle) grains deposited in the Barents Sea basin during the Latest Triassic is the occurrence of rounded quartz overgrowths with high homogenization temperatures in the recycled portion.

Our data strongly supports the current hypothesis of large-scale sedimentary recycling associated with the uplift of the Novaya Zemlya Archipelago during the latest Triassic. Unlike petrographic, geochemical and geochronological provenance investigations of Triassic-Jurassic successions on the Barents Shelf (Fleming et al., 2016; Khudoley et al., 2019; Klausen et al., 2017; Line et al., 2020), the combined approach applied herein is able to identify basin-scale sedimentary recycling.

General implications

Grains with inherited quartz cement are a reoccurring component in siliciclastic sandstone (e.g., Johnsson et al., 1988; Ulmer-Scholle et al., 2014). Recycled sedimentary particles count amongst the greatest challenges in petrographic interpretations of sandstones (Blatt, 1967) and much work remains to detect recycling in the sedimentary rock record. Provenance studies that assume direct transport from crystalline source rocks and neglect sediment recycling as viable possibility can be balanced by the detection of recycled components. As such, identification and quantification of recycled sedimentary particles represent important input for a variety of research disciplines, including reservoir quality assessment, basin stratigraphy reconstructions, provenance reconstructions, basin infill modelling and source-to-sink analysis. The combined use of surface textures and fluid inclusion analysis of authigenic quartz overgrowths can offer new opportunities for evaluating the geological record.

Tectonic reconfigurations have crucial implications for sediment routing patterns and the thermal evolution of the sedimentary basin infill – both in the studied succession and other foreland basins situated in equally complex structural settings. Whilst the consequences of sediment recycling for source-to-sink analyses are thoroughly assessed in the literature (e.g., Andersen et al., 2016; Blatt, 1967), implications of sediment burial and resulting thermal history implied by the tectonic reconstructions are largely ignored. Failure to notice recycled grains in sedimentary successions may have serious consequences for diagenetic modelling as inherited quartz cement might be regarded as *in-situ* cement affiliated with the last burial cycle of the host sediment. Such misidentification can easily lead to overestimation of quartz cement volume, resulting in incorrect thermal history reconstructions and flawed uplift estimates. Ultimately, compaction and cementation models employed in reservoir quality predictions and basin modelling may be compromised (Gallagher & Parra, 2020; Walderhaug, 1996; Worden et al., 2018). Most sedimentary basins worldwide are susceptible to sediment supply from older and uplifted sedimentary rocks indicating that inherited quartz cement is a global issue. Therefore, burial history reconstruction and reservoir quality prediction should be handled cautiously.

Fluid inclusion microthermometry of rounded syntaxial quartz overgrowths exerts constraints on the lithology and thermal history of sedimentary provenance terrain(s) as complement to conventional geochemical and geochronological analyses of detrital grains. Recycled syntaxial quartz overgrowths can only originate from exposed sedimentary rock, whereas detrital grains often carry characteristic imprints from their igneous and metamorphic proto sources (Miller, Gehrels, Pease, & Sokolov, 2010; von Eynatten & Dunkl, 2012). If regional geothermal gradients of a sedimentary basin are known, measured homogenization temperatures in quartz overgrowths may also constrain the burial history and uplift magnitude of the precursor sedimentary basin.

The methods employed herein only applies to quartz grains that have been subjected to burial depths at which temperatures exceeded ~70°C. Recycled grains without syntaxial quartz overgrowths bear no diagnostic imprint of previous burial sequences and cannot provide indications of polycyclic origin (von Eynatten & Dunkl, 2012). Although presented as a case study from the western Barents Sea basin, the combination of single-grain techniques employed herein is generally applicable and can be used to identify recycled components in sedimentary basins worldwide. Whilst applicable to all types of quartz bearing siliciclastic sandstone, the proposed multidisciplinary approach is particularly suited for quartz arenitic sandstones where quartz grains constitute one of the sole means for unravelling the sediment history (Blatt, 1967).

CONCLUSIONS

- The diagenetic imprints from the Lower Mesozoic strata in the Barents Sea basin imply delivery of significant amount of recycled sediments from an uplifted sedimentary paleo-basin with regional-scale sediment dispersal potential.
- We have demonstrated the potential of coupling petrography and cathodoluminescence characteristics of quartz overgrowths integrated with fluid inclusion microthermometry to impose additional constraints on the provenance of recycled grains. This combined approach can also constrain the burial depth in the subsequently inverted sedimentary basin.
- Failure to identify sedimentary recycling may have serious consequences for diagenetic modelling, where thermal history reconstructions, uplift estimations, compaction and

cementation modelling and reservoir quality predictions may be compromised. Identification of recycled sediment can eventually lead to a more complete understanding of the basin infill history and source to sink relationships.

- The novel multidisciplinary approach presented herein can also be used in constraining sediment recycling in sedimentary basins worldwide that are susceptible to quartz-rich sediment supply from older uplifted and exposed sedimentary basins.

REFERENCES CITED

Andersen, T., Kristoffersen, M., & Elburg, M. A. (2016). How far can we trust provenance and crustal evolution information from detrital zircons? A South African case study. *Gondwana Research, 34*, 129-148.

Anell, I., Faleide, J.I, & Braathen, A. (2016). Regional tectono-sedimentary development of the highs and basins of the northwestern Barents Shelf. Norsk Geologisk Tidsskrift, 96, 27-41.

Anell, I., Thybo, H., & Artemieva, I. (2009). Cenozoic uplift and subsidence in the North Atlantic region: Geological evidence revisited. *Tectonophysics, 474*(1-2), 78-105.

Anell, I. M., Braathen, A., & Olaussen, S. (2014). The Triassic–Early Jurassic of the northern Barents Shelf: a regional understanding of the Longyearbyen CO_2 reservoir. *Norsk Geologisk Tidsskrift, 94*, 83-98.

Augustsson, C., Rusing, T., Adams, C. J., Chmiel, H., Kocabayoglu, M., Buld, M., . . . Kooijman, E. (2011). Detrital quartz and zircon combined: The production of mature sand with short transportation paths along the Cambrian west Gondwana margin, northwestern Argentina. *Journal of Sedimentary Research, 81*(4), 284-298.

Austin, G. S. (1974). Multiple overgrowths on detrital quartz sand grains in the Shakopee Formation (Lower Ordovician) of Minnesota. Journal of Sedimentary Research, 44(2), 358-362.

Baig, I., Faleide, J. I., Jahren, J., & Mondol, N. H. (2016). Cenozoic exhumation on the southwestern Barents Shelf: Estimates and uncertainties constrained from compaction and thermal maturity analyses. Marine and Petroleum Geology, 73, 105-130. doi:https://doi.org/10.1016/j.marpetgeo.2016.02.024

Basu, A., Schieber, J., Patranabis-Deb, S., & Dhang, P. C. (2013). Recycled detrital quartz grains are sedimentary rock fragments indicating unconformities: examples from the Chhattisgarh Supergroup, Bastar Craton, India. *Journal of Sedimentary Research, 83*(4), 368-376.

Bergan, M., & Knarud, R. (1993). Apparent changes in clastic mineralogy of the Triassic–Jurassic succession, Norwegian Barents Sea: possible implications for palaeodrainage and subsidence. In *Norwegian Petroleum Society Special Publications* (Vol. 2, pp. 481-493): Elsevier.

Bjørlykke, K., & Egeberg, P. (1993). Quartz cementation in sedimentary basins. *AAPG bulletin, 77*(9), 1538-1548.

Blatt, H. (1967). Provenance determinations and recycling of sediments. *Journal of Sedimentary Research, 37*(4), 1031-1044.

Bodnar, R. J. (2003a). Introduction to fluid inclusions. In I. Samson, A. Anderson, & D. Marshall (Eds.), *Fluid inclusions: Analysis and interpretation* (Vol. 32, pp. 1-8): Mineralogical Association of Canada, Short course.

Bodnar, R. J. (2003b). Reequilibration of fluid inclusions. In I. Samson, A. Anderson, & D. Marshall (Eds.), *Fluid inclusions: Analysis and interpretation* (Vol. 32, pp. 213-230): Mineralogical Association of Canada, Short Course.

Bouch, J. E., Hole, M. J., Trewin, N. H., Chenery, S., & Morton, A. C. (2002). Authigenic apatite in a fluvial sandstone sequence: evidence for rare-earth element mobility during diagenesis and a tool for diagenetic correlation. *Journal of Sedimentary Research, 72*(1), 59-67.

Braathen, A., Bælum, K., Christiansen, H. H., Dahl, T., Eiken, O., Elvebakk, H., . . . Johansen, T. A. (2012). The Longyearbyen CO_2 Lab of Svalbard, Norway—initial assessment of the geological conditions for CO_2 sequestration. *Norwegian Journal of Geology, 92*(4), 353-376.

Bue, E. P., & Andresen, A. (2014). Constraining depositional models in the Barents Sea region using detrital zircon U–Pb data from Mesozoic sediments in Svalbard. *Geological Society, London, Special Publications, 386*(1), 261-279.

Burley, S., Mullis, J., & Matter, A. (1989). Timing diagenesis in the Tartan Reservoir (UK North Sea): constraints from combined cathodoluminescence microscopy and fluid inclusion studies. Marine and Petroleum Geology, 6(2), 98-120.

Caja Rodríguez, M. Á., Marfil, R., Estupiñán Letamendi, J., Morad, S., Mansurbeg, H., García, D., & Amorosi, A. (2008). Diagenesis and porosity evolution of Cretaceous turbidite sandstones: Vøring Basin, mid-Norway passive margin. Geotemas, 10, 1441-1444.

Campbell, I. H., Reiners, P. W., Allen, C. M., Nicolescu, S., & Upadhyay, R. (2005). He–Pb double dating of detrital zircons from the Ganges and Indus Rivers: implication for quantifying sediment recycling and provenance studies. *Earth and Planetary Science Letters, 237*(3-4), 402-432.

Cooper, M., Evans, J., Flint, S., Hogg, A., & Hunter, R. (2000). Quantification of detrital, authigenic and porosity components of the Fontainebleau Sandstone: a comparison of conventional optical and combined scanning electron microscope-based methods of modal analyses. IAS-Special Publication, 29, 89-102. doi:https://doi.org/10.1002/9781444304237.ch7

Doré, A. (1991). The structural foundation and evolution of Mesozoic seaways between Europe and the Arctic. Palaeogeography, Palaeoclimatology, Palaeoecology, 87(1-4), 441-492.

Dott, J., RH. (2003). The importance of eolian abrasion in supermature quartz sandstones and the paradox of weathering on vegetation-free landscapes. *The Journal of Geology, 111*(4), 387-405.

Drachev, S. S. (2016). Fold belts and sedimentary basins of the Eurasian Arctic. *Arktos, 2*(1), 21-30.

Faleide, J. I., Pease, V., Curtis, M., Klitzke, P., Minakov, A., Scheck-Wenderoth, M., . . . Zayonchek, A. (2018). Tectonic implications of the lithospheric structure across the Barents and Kara shelves. *Geological Society, London, Special Publications, 460*(1), 285-314.

Faleide, J. I., Vågnes, E., & Gudlaugsson, S. T. (1993). Late Mesozoic-Cenozoic evolution of the south-western Barents Sea in a regional rift-shear tectonic setting. Marine and Petroleum Geology, 10(3), 186-214.

Fleming, E. J., Flowerdew, M. J., Smyth, H. R., Scott, R. A., Morton, A. C., Omma, J. E., . . . Whitehouse, M. J. (2016). Provenance of Triassic sandstones on the southwest Barents Shelf and the implication for sediment dispersal patterns in northwest Pangaea. *Marine and Petroleum Geology, 78*, 516-535.

Gallagher, K., & Parra, M. (2020). A new approach to thermal history modelling with detrital low temperature thermochronological data. *Earth and Planetary Science Letters, 529*, 115872. doi:https://doi.org/10.1016/j.epsl.2019.115872

Glørstad-Clark, E., Faleide, J. I., Lundschien, B. A., & Nystuen, J. P. (2010). Triassic seismic sequence stratigraphy and paleogeography of the western Barents Sea area. *Marine and Petroleum Geology, 27*(7), 1448-1475.

Goldstein, R. H. (2001). Fluid inclusions in sedimentary and diagenetic systems. Lithos, 55(1-4), 159-193.

Golonka, J. (2007). Late Triassic and Early Jurassic palaeogeography of the world. *Palaeogeography, Palaeoclimatology, Palaeoecology, 244*(1-4), 297-307.

Golonka, J., Embry, A., & Krobicki, M. (2018). Late triassic global plate tectonics. In H. T. Lawrence (Ed.), *The late triassic world. Topics in Geobiology* (Vol. 46, pp. 27-57): Springer, Cham.

Götte, T. (2018). Trace element composition of authigenic quartz in sandstones and its correlation with fluid–rock interaction during diagenesis. Geological Society, London, Special Publications, 435(1), 373-387.

Götte, T., & Richter, D. K. (2006). Cathodoluminescence characterization of quartz particles in mature arenites. *Sedimentology, 53*(6), 1347-1359.

Haile, B. G., Czarniecka, U., Xi, K., Smyrak-Sikora, A., Jahren, J., Braathen, A., & Hellevang, H. (2019). Hydrothermally induced diagenesis: Evidence from shallow marine-deltaic sediments, Wilhelmøya, Svalbard. *Geoscience Frontiers, 10*(2), 629-649.

Haile, B. G., Klausen, T. G., Jahren, J., Braathen, A., & Hellevang, H. (2018). Thermal history of a Triassic sedimentary sequence verified by a multi-method approach: Edgeøya, Svalbard, Norway. *Basin Research, 30*(6), 1075-1097.

Henriksen, E., Bjørnseth, H., Hals, T., Heide, T., Kiryukhina, T., Kløvjan, O., . . . Sollid, K. (2011). Uplift and erosion of the greater Barents Sea: impact on prospectivity and petroleum systems. *Geological Society, London, Memoirs, 35*(1), 271-281.

Henry, D. J., & Dutrow, B. L. (1992). Tourmaline in a low grade clastic metasedimentary rock: an example of the petrogenetic potential of tourmaline. *Contributions to Mineralogy and Petrology, 112*(2-3), 203-218.

Hollister, L., Crawford, M., Roedder, E., Burruss, R., Spooner, E., & Touret, J. (1981). Practical aspects of microthermometry. *Fluid Inclusions: Applications to Petrology, 6*, 13-38.

Johnsson, M. (1993). The system controlling the composition of clastic sediments. In M. Johnsson & A. Basu (Eds.), Process Controlling the Composition of Clastic Sediment;Boulder, Colorado,. *Special Papers-Geological Society of America*, 284, 1-20.

Johnsson, M. J., Stallard, R. F., & Meade, R. H. (1988). First-cycle quartz arenites in the Orinoco River basin, Venezuela and Colombia. *The Journal of Geology, 96*(3), 263-277.

Khudoley, A. K., Sobolev, N. N., Petrov, E. O., Ershova, V. B., Makariev, A. A., Makarieva, E. V., . . . Sobolev, P. O. (2019). A reconnaissance provenance study of Triassic–Jurassic clastic rocks of the Russian Barents Sea. *GFF*, 1-9.

Klausen, T. G., Müller, R., Poyatos-Moré, M., Olaussen, S., & Stueland, E. (2019). Tectonic, provenance and sedimentological controls on reservoir characteristics in the Upper Triassic to Middle Jurassic Realgrunnen Subgroup – Southwest Barents Sea. *Geological Society, London, Special Publications, 495*, SP495-2018-2165. doi:10.1144/sp495-2018-165

Klausen, T. G., Müller, R., Slama, J., & Helland-Hansen, W. (2017). Evidence for Late Triassic provenance areas and Early Jurassic sediment supply turnover in the Barents Sea Basin of northern Pangea.

Klausen, T. G., Ryseth, A. E., Helland-Hansen, W., Gawthorpe, R., & Laursen, I. (2014). Spatial and temporal changes in geometries of fluvial channel bodies from the Triassic Snadd Formation of offshore Norway. *Journal of Sedimentary Research, 84*(7), 567-585.

Land, L. S., & Fisher, R. S. (1987). Wilcox sandstone diagenesis, Texas Gulf Coast: a regional isotopic comparison with the Frio Formation. *Geological Society, London, Special Publications, 36*(1), 219-235.

Lehmann, K., Pettke, T., & Ramseyer, K. (2011). Significance of trace elements in syntaxial quartz cement, Haushi Group sandstones, Sultanate of Oman. Chemical geology, 280(1-2), 47-57.

Line, L. H., Reidar, M., Tore, G. K., Jens, J., & Helge, H. (2020). Distinct petrographic responses to basin reorganization across the Triassic–Jurassic boundary in the southwestern Barents Sea. *Basin Research*. *https://doi.org/10.1111/bre.12437*.

Lord, G. S., Mørk, M. B. E., Mørk, A., & Olaussen, S. (2019). Sedimentology and petrography of the Svenskøya Formation on Hopen, Svalbard: an analogue to sandstone reservoirs in the Realgrunnen Subgroup. *Polar Research, 38*, 10.33265/polar. v33238. 33523.

McLennan, S. M., & Taylor, S. (1980). Th and U in sedimentary rocks: crustal evolution and sedimentary recycling. *Nature, 285*(5767), 621-624.

Meinhold, G. (2010). Rutile and its applications in earth sciences. *Earth-Science Reviews, 102*(1-2), 1-28.

Miller, E., Gehrels, G., Pease, V., & Sokolov, S. J. A. b. (2010). Stratigraphy and U-Pb detrital zircon

geochronology of Wrangel Island, Russia: Implications for Arctic paleogeography. *94*(5), 665-692.
Moecher, D., Kelly, E., Hietpas, J., & Samson, S. D. (2019). Proof of recycling in clastic sedimentary systems from textural analysis and geochronology of detrital monazite: Implications for detrital mineral provenance analysis. *Bulletin, 131*(7-8), 1115-1132.
Morad, S., Ketzer, J., & De Ros, L. F. (2000). Spatial and temporal distribution of diagenetic alterations in siliciclastic rocks: implications for mass transfer in sedimentary basins. Sedimentology, 47, 95-120.
Morton, A., & Hurst, A. (1995). Correlation of sandstones using heavy minerals: an example from the Statfjord Formation of the Snorre Field, northern North Sea. *Geological Society, London, Special Publications, 89*(1), 3-22.
Mulrooney, M. J., Rismyhr, B., Yenwongfai, H. D., Leutscher, J., Olaussen, S., Braathen, A. J. M., & Geology, P. (2018). Impacts of small-scale faults on continental to coastal plain deposition: Evidence from the Realgrunnen Subgroup in the Goliat field, southwest Barents Sea, Norway. *95*, 276-302.
Müller, R., Klausen, T., Faleide, J., Olaussen, S., Eide, C., & Suslova, A. (2019). Linking regional unconformities in the Barents Sea to compression-induced forebulge uplift at the Triassic-Jurassic transition. *Tectonophysics*, 765, 35-51. https://doi.org/10.1016/j.tecto.2019.04.006
Mørk, A., & Bjorøy, M. (1984). Mesozoic source rocks on Svalbard. In A. M. Spencer, E. Holter, A. Johnsen, A. Mørk, E. Nysæther, P. Songstad, & Spinnangr (Eds.), *Petroleum geology of the North European margin* (pp. 371-382). London: Graham and Trotman.
Mørk, A., Dallmann, W., Dypvik, H., Johannessen, E., Larssen, G., Nagy, J., . . . Worsley, D. (1999). Mesozoic lithostratigraphy. In W. Dallmann (Ed.), *Lithostratigraphic Lexicon of Svalbard: Upper Palaeozoic to Quaternary bedrock. Review recommendations for nomenclature use* (pp. 127-214). Tromsø, Norway: Norwegain Polar Institute.
Mørk, M. B. E. (1999). Compositional variations and provenance of Triassic sandstones from the Barents Shelf. *Journal of Sedimentary Research, 69*(3), 690-710.
Najman, Y. (2006). The detrital record of orogenesis: A review of approaches and techniques used in the Himalayan sedimentary basins. *Earth-Science Reviews, 74*(1-2), 1-72.
Nyland, B., Jensen, L., Skagen, J., Skarpnes, O., & Vorren, T. (1992). Tertiary uplift and erosion in the Barents Sea: magnitude, timing and consequences. In *Structural and tectonic modelling and its application to petroleum geology* (pp. 153-162): Elsevier.
Oelkers, E. H., Bjørkum, P. A., Walderhaug, O., Nadeau, P. H., & Murphy, W. M. (2000). Making diagenesis obey thermodynamics and kinetics: the case of quartz cementation in sandstones from offshore mid-Norway. *Applied Geochemistry, 15*(3), 295-309.
Oelkers, E. H., Bjørkum, P. A., & Murphy, W. M. (1996). A petrographic and computational investigation of quartz cementation and porosity reduction in North Sea sandstones. American Journal of Science, 296, 420-452.
Ohm, S. E., Karlsen, D. A., & Austin, T. (2008). Geochemically driven exploration models in uplifted areas: Examples from the Norwegian Barents Sea. *AAPG bulletin, 92*(9), 1191-1223.
Olaussen, S., Dalland, A., Gloppen, T., & Johannessen, E. (1984). Depositional environment and diagenesis of Jurassic reservoir sandstones in the eastern part of Troms I area. In A. M. Spencer (Ed.), *Petroleum Geology of the North European Margin* (pp. 61-79): Springer.
Olaussen, S., Larssen, G. B., Helland-Hansen, W., Johannessen, E. P., Nøttvedt, A., Riis, F., . . . Worsley, D. (2018). Mesozoic strata of Kong Karls Land, Svalbard, Norway; a link to the northern Barents Sea basins and platforms. *Norwegian Journal of Geology/Norsk Geologisk Forening, 98*(4), 1-69.
Pease, V. (2011). Eurasian orogens and Arctic tectonics: an overview. *Geological Society, London, Memoirs, 35*(1), 311-324.
Ramm, M., Forsberg, A. W., & Jahren, J. S. (1997). Porosity--Depth Trends in Deeply Buried Upper

Jurassic Reservoirs in the Norwegian Central Graben: An Example of Porosity Preservation Beneath the Normal Economic Basement by Grain-Coating Microquartz. In Kupecz, J. A., Gluyas, J., and Bloch,S. (Ed.),. Reservoir Quality Prediction in Sandstones and Carbonates, AAPG Memoir 69, 117-199.

Rezaee, M. R., & Tingate, P. R. (1997). Origin of quartz cement in the Tirrawarra sandstone, southern Cooper basin, South Australia. Journal of Sedimentary Research, 67(1), 168-177.

Richter, D., Götte, T., Götze, J., & Neuser, R. (2003). Progress in application of cathodoluminescence (CL) in sedimentary petrology. *Mineralogy and Petrology, 79*(3-4), 127-166.

Rismyhr, B., Bjærke, T., Olaussen, S., Mulrooney, M. J., & Senger, K. (2019). Facies, palynostratigraphy and sequence stratigraphy of the Wilhelmøya Subgroup (Upper Triassic–Middle Jurassic) in western central Spitsbergen, Svalbard. Norwegian Journal of Geology, 35-64. doi:https://dx.doi.org/10/17850/njg001

Roedder, E. (1984). Fluid inclusions. Rev. Mineralogy, *Mineralogical Society of America, v. 12, 644 p*.

Ryseth, A. (2014). Sedimentation at the Jurassic–Triassic boundary, south-west Barents Sea: indication of climate change. In A. W. Martinius, R. Ravnås, J. A. Howell, R. J. Steel, & J. P. Wonham (Eds.), *From Depositional Systems to Sedimentary Successions on the Norwegian Continental Margin* (Vol. 46, pp. 187-214): IAS, Willey Blackwell.

Sanderson, I. D. (1984). Recognition and significance of inherited quartz overgrowths in quartz arenites. *Journal of Sedimentary Research, 54*(2), 473-486.

Sobolev, P. (2012). Cenozoic uplift and erosion of the Eastern Barents Sea–constraints from offshore well data and the implication for petroleum system modelling. *Zeitschrift der Deutschen Gesellschaft für Geowissenschaften, 163*(3), 309-324.

Sømme, T., Doré, A., Lundin, E., & Tørudbakken, B. J. A. B. (2018). Triassic–Paleogene paleogeography of the Arctic: Implications for sediment routing and basin fill. AAPG Bulletin, *102*(12), 2481-2517.

Toro, J., Miller, E., Prokopiev, A., Zhang, X., & Veselovskiy, R. (2016). Mesozoic orogens of the Arctic from Novaya Zemlya to Alaska. *journal of the Geological Society, 173*(6), 989-1006.

Tyrrell, S., Leleu, S., Souders, A. K., Haughton, P. D., & Daly, J. S. (2009). K‐feldspar sand‐grain provenance in the Triassic, west of Shetland: distinguishing first-cycle and recycled sediment sources? *Geological Journal, 44*(6), 692-710.

Ulmer-Scholle, D. S., Scholle, P. A., Schieber, J., & Raine, R. J. (2014). A color guide to the petrography of sandstones, siltstones, shales and associated rocks: American Association of Petroleum Geologists Memoir, 562pp.

Von Eynatten, H., & Dunkl, I. (2012). Assessing the sediment factory: the role of single grain analysis. *Earth-Science Reviews, 115*(1-2), 97-120.

Walderhaug, O. (1994). Temperatures of quartz cementation in Jurassic sandstones from the Norwegian continental shelf; evidence from fluid inclusions. *Journal of Sedimentary Research, 64*(2a), 311-323.

Walderhaug, O. (1996). Kinetic modeling of quartz cementation and porosity loss in deeply buried sandstone reservoirs. *AAPG bulletin, 80*(5), 731-745.

Walderhaug, O., & Bjørkum, P. A. (2003). The effect of stylolite spacing on quartz cementation in the Lower Jurassic Stø Formation, southern Barents Sea. *Journal of Sedimentary Research, 73*(2), 146-156.

Worden, R., Armitage, P., Butcher, A., Churchill, J., Csoma, A., Hollis, C., . . . Omma, J. (2018). Petroleum reservoir quality prediction: overview and contrasting approaches from sandstone and carbonate communities. *Geological Society, London, Special Publications, 435*(1), 1-31.

Worden, R., & Burley, S. (2003). Sandstone diagenesis: the evolution of sand to stone. In S. Burley & R. Worden (Eds.), *Sandstone Diagenesis: Recent and Ancient* (Vol. 4, pp. 3-44). UK: Blackwell Publishing Ltd.

Worden, R., & Morad, S. (2000). Quartz cementation in oil field sandstones: a review of the key controversies. Special Publication-International Association of Sedimentologists, 29, 1-20.

Worsley, D. (2008). The post-Caledonian development of Svalbard and the western Barents Sea. *Polar*

Research, 27(3), 298-317.

Worsley, D., Johansen, R., & Kristensen, S. (1988). The mesozoic and cenozoic succession of Tromsøflaket. A lithostratigraphic scheme for the Mesozoic and Cenozoic succession offshore mid-and northern Norway. Norwegian Petroleum Directorate Bulletin, 4, 42-65.

Zhang, X., Pease, V., Carter, A., & Scott, R. (2018). Reconstructing Palaeozoic and Mesozoic tectonic evolution of Novaya Zemlya: combing geochronology and thermochronology. Geological Society, London, Special Publications, 460(1), 335-353.

Ziegler, P. (1988). Post-Hercynian plate reorganization in the Tethys and Arctic–North Atlantic domains. In Developments in Geotectonics (Vol. 22, pp. 711-755): Elsevier.

TABLE CAPTION

Table 1. Locations of studied samples from the western Barents Sea basin with estimated maximum burial depths.

FIGURE CAPTIONS

Figure 1. A) Simplified schematic map of the arctic showing the Barents Sea basin surrounded by major tectonic terranes and the sampling locations. B) Lithostratigraphic chart of the Mesozoic sedimentary units (after Mørk et al., 1999 and Lord et al. 2019). The sampled sedimentary intervals are marked with red circles.

Figure 2. A) Micrographs of detrital quartz grains with (red arrows) rounded quartz overgrowths under plane polarized light, Svenskøya Formation. B) SEM-CL micrographs of detrital quartz grains with (red arrows) rounded quartz overgrowths, Svenskøya Formation. C) Close up of detrital quartz grain with inherited authigenic rounded quartz overgrowths delineated by dust rims. D) Fluid inclusion homogenization temperatures for inherited authigenic rounded quartz overgrowths of Wilhelmøya Subgroup (Flatsalen and Svenskøya formations) sediment from northeast Svalbard (Wilhelmøya). The location of outcrop samples is eastern Wilhelmøya (79.06825°N and 20.72986°E, 79.08144°N and 20.68276 °E).

Figure 3. Representative detrital quartz grain from the Wilhelmøya Subgroup (Svenskøya Formation) with well-rounded and abraded quartz overgrowth, coated with microcrystalline

quartz. A) SEM secondary electron micrograph. B) SEM-CL micrograph illustrating thin rounded quartz overgrowth (darker CL intensity than the detrital quartz grain). C) Close-up part of the quartz grain in Figure 3B (red rectangle) with rounded but also spalled off quartz overgrowths coated with a thin layer of microcrystalline quartz. The location of outcrop sample is eastern Wilhelmøya (79.06825°N and 20.72986°E).

Figure 4. Representative SEM-CL micrographs. A) Realgrunnen Subgroup (Stø Formation, ~717 m of current burial depth) samples contain substantial amounts of detrital quartz grains rimmed with rounded quartz overgrowths (red arrows). B) Penetrating overgrowths at sutured contact (red arrows), Fruholmen Formation (current burial depth of ~752.7 m). C-D) Grayscale and RGB micrographs with double quartz overgrowths on detrital quartz grains, Stø Formation. The inner overgrowth (g1) is zoned and lighter gray than the outer one (g2). QD = detrital quartz, QO = quartz overgrowths.

Figure 5. Schematic representation of the observed microscale properties in quartz, showing records of diagenetic fingerprints. A) inherited overgrowths (dark grey) with rounded edges and corroded surface textures due to transport and chemical weathering and authigenic/*in situ* quartz (light grey) with euhedral crystal interfaces, B) sutured intergranular contact of detrital quartz grains with authigenic quartz overgrowths (dark grey). Mutual interpenetration often is accompanied by quartz precipitation at adjacent free grain surfaces (light grey) rather than at the intergranular grain contact itself. C) Double quartz overgrowths and microquartz coatings (black) on rounded quartz overgrowth, and D) trapped fluid inclusions along with homogenization temperatures for *in situ* (white dots) and recycled (grey dots) quartz overgrowths when inherited quartz overgrowths indicate higher thermal history than the host sediment.

Figure 6. Proposed conceptual model for the sediment routing on the Barents Sea basin during Triassic-Jurassic time. The model based on data from this study and published seismic,

sedimentological, geochronological and paleogeographic reconstruction data (Bergan & Knarud, 1993; Bue & Andresen, 2014; Fleming et al., 2016; Glørstad-Clark et al., 2010; Klausen et al., 2017; Müller et al., 2019; Mørk, 1999; Sømme, Doré, Lundin, & Tørudbakken, 2018). **A)** Before thrusting-up of Novaya Zemlya most of Triassic time. **B)** Latest Triassic.

NZFTB = Novaya Zemlya Fold and Thrust Belt

Figure 1

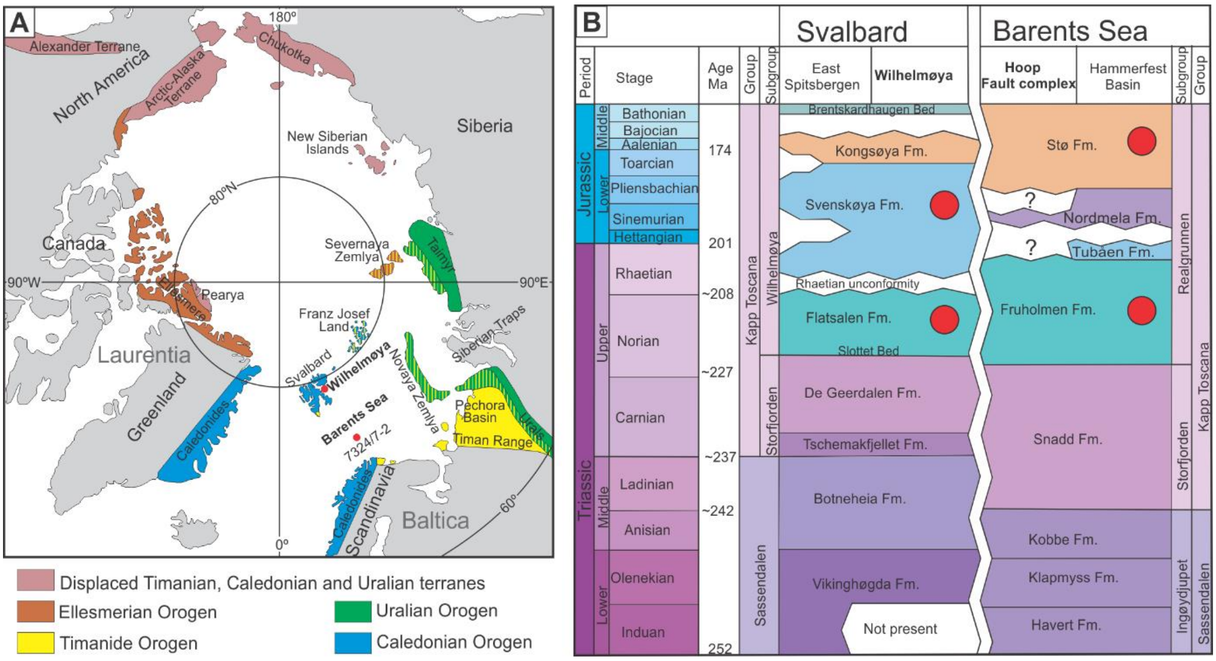

Figure 2

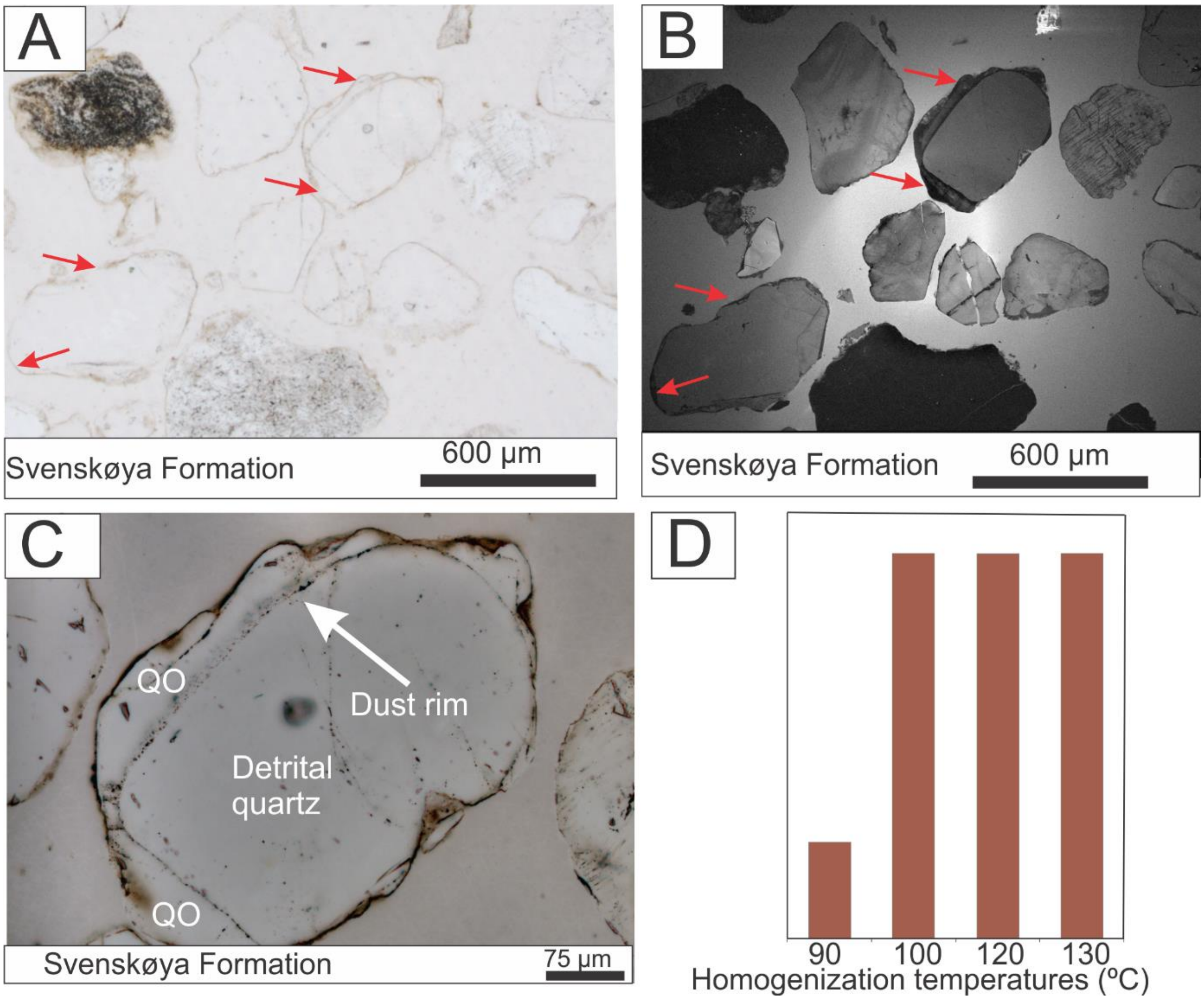
A
Svenskøya Formation
600 µm
B
Svenskøya Formation
600 µm
C
QO
Dust rim
Detrital quartz
QO
Svenskøya Formation
75 µm
D
90
100
120
130
Homogenization temperatures (ºC)

Figure 3

757

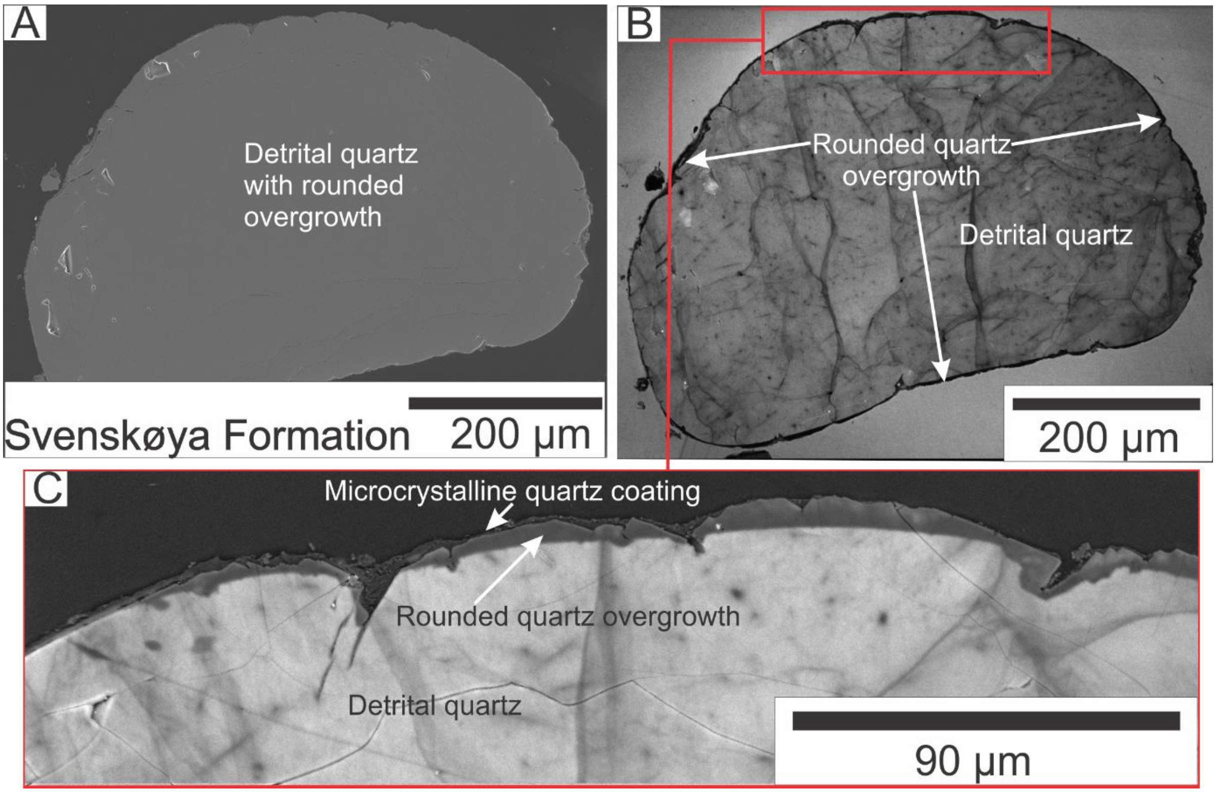

758 Figure 4

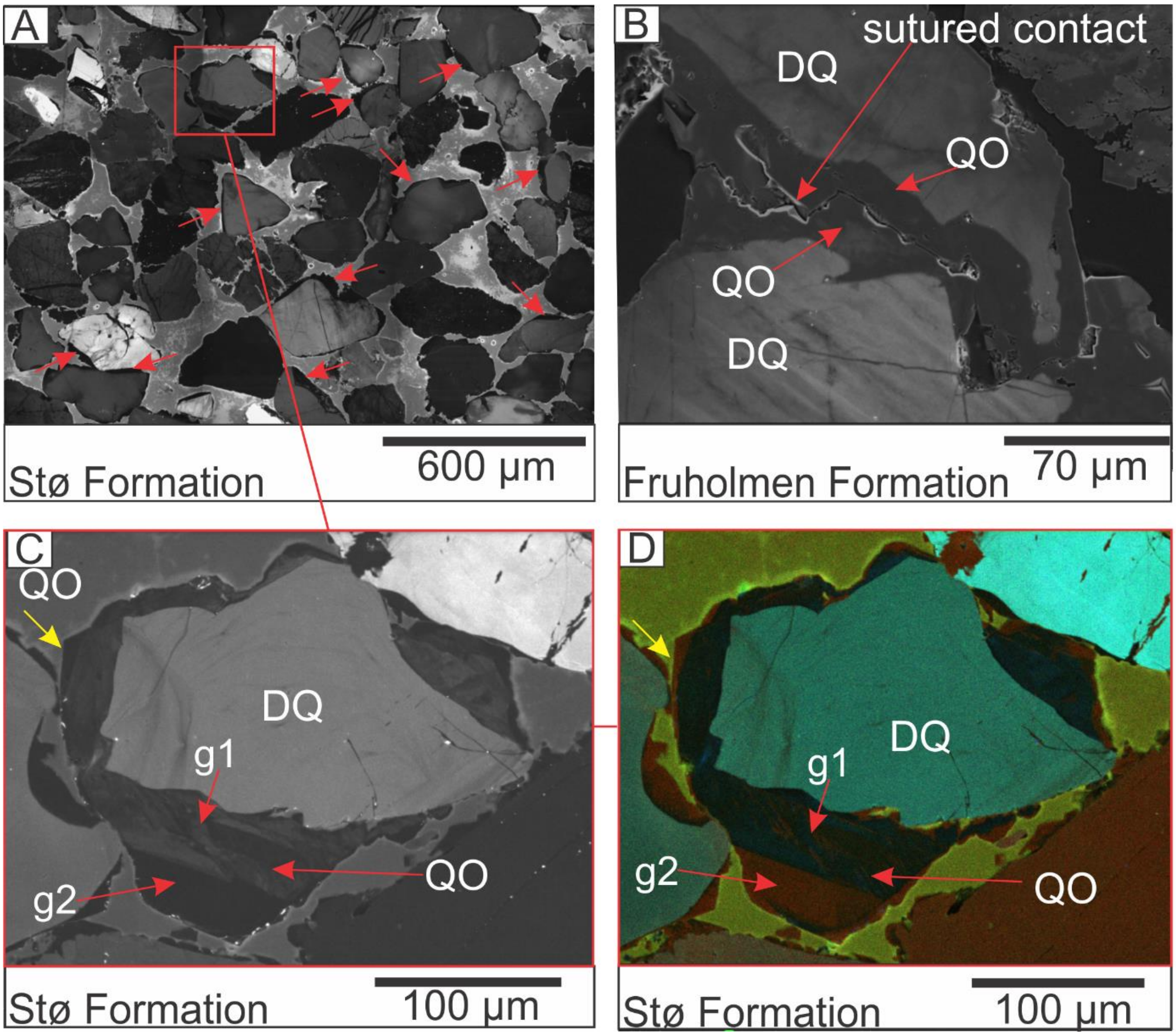
A
Stø Formation
600 µm
B
sutured contact
DQ
QO
QO
DQ
Fruholmen Formation
70 µm
C
QO
DQ
g1
g2
QO
Stø Formation
100 µm
D
DQ
g1
g2
QO
Stø Formation
100 µm

Figure 5

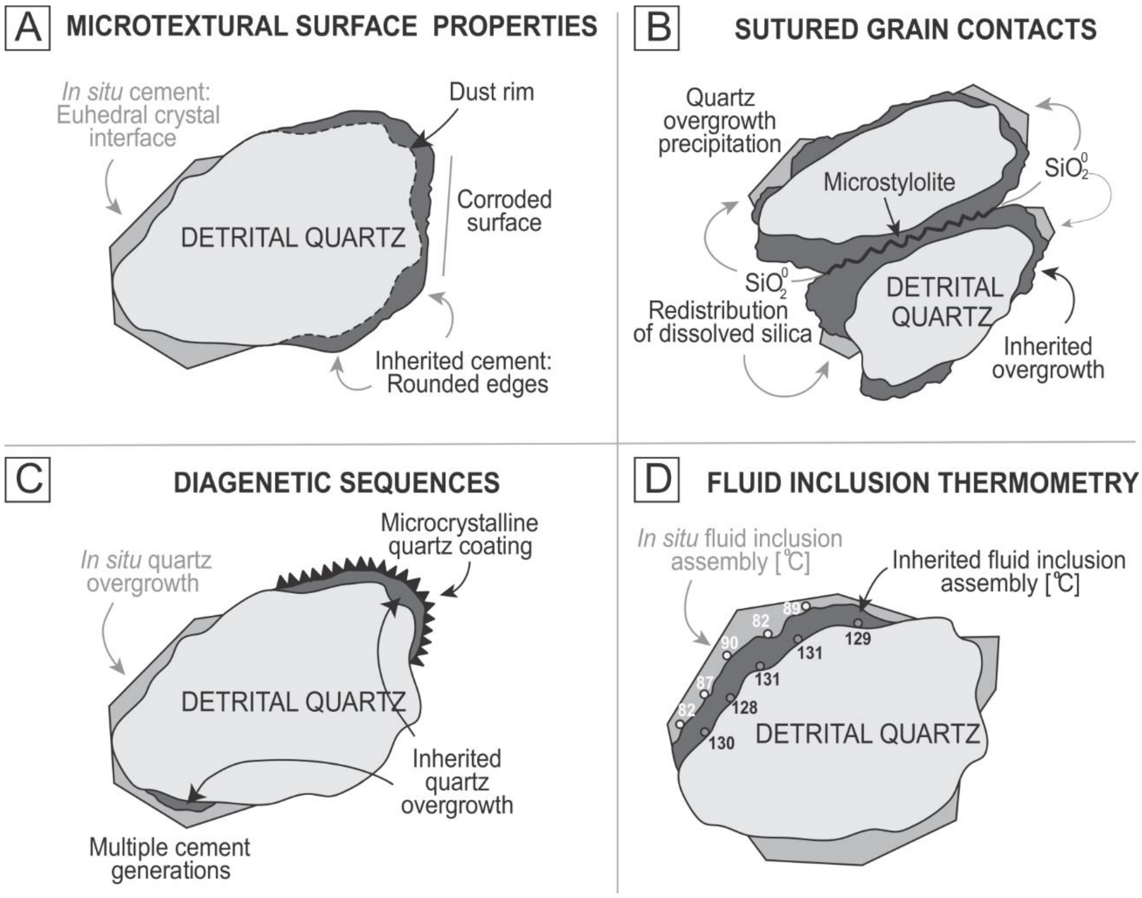

A MICROTEXTURAL SURFACE PROPERTIES
In situ cement: Euhedral crystal interface
Dust rim
Corroded surface
DETRITAL QUARTZ
Inherited cement: Rounded edges
B SUTURED GRAIN CONTACTS
Quartz overgrowth precipitation
Microstylolite
SiO_2^0
SiO_2^0
Redistribution of dissolved silica
DETRITAL QUARTZ
Inherited overgrowth
C DIAGENETIC SEQUENCES
In situ quartz overgrowth
Microcrystalline quartz coating
DETRITAL QUARTZ
Inherited quartz overgrowth
Multiple cement generations
D FLUID INCLUSION THERMOMETRY
In situ fluid inclusion assembly [℃]
Inherited fluid inclusion assembly [℃]
89
82
90
87
82
129
131
131
128
130
DETRITAL QUARTZ

Figure 6

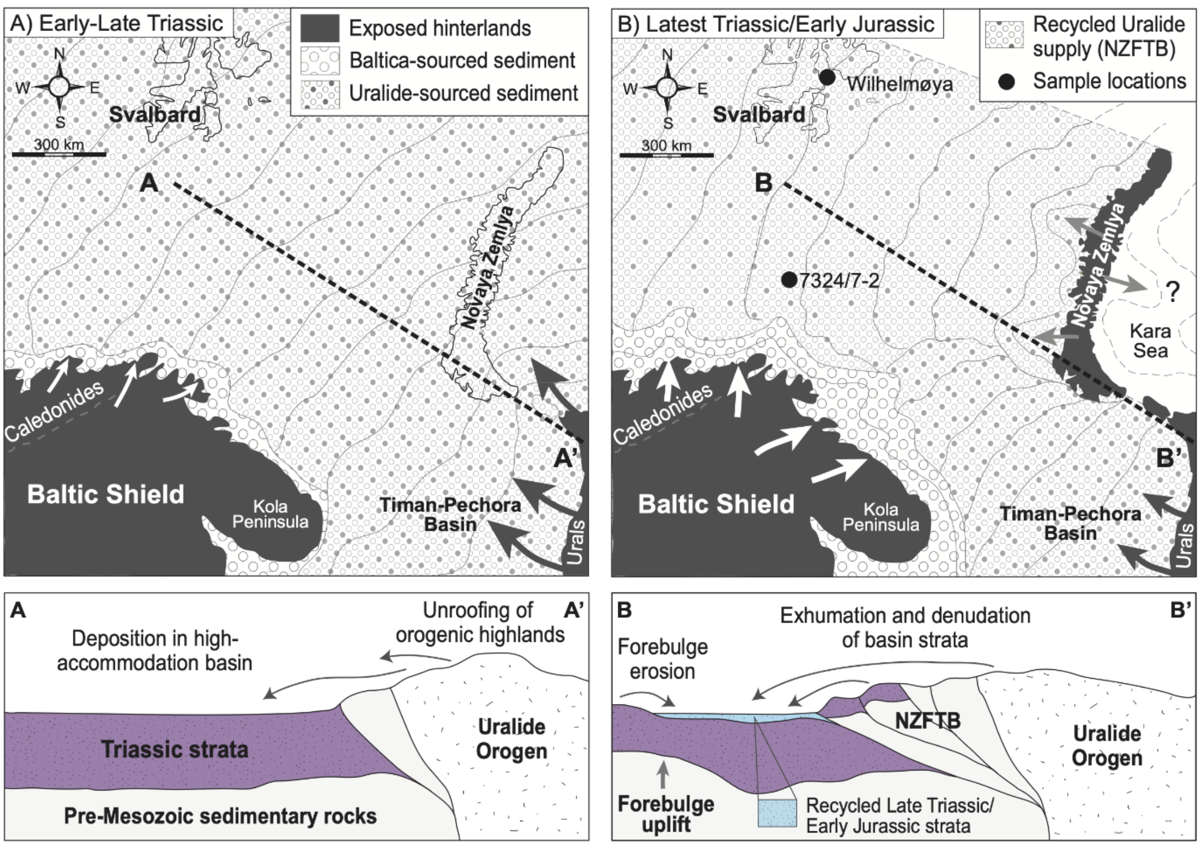

A) Early-Late Triassic
Exposed hinterlands
Baltica-sourced sediment
Uralide-sourced sediment
N
W
E
S
Svalbard
300 km
A
Novaya Zemlya
Caledonides
A'
Baltic Shield
Kola Peninsula
Timan-Pechora Basin
Urals
B) Latest Triassic/Early Jurassic
Recycled Uralide supply (NZFTB)
Sample locations
Wilhelmøya
Svalbard
300 km
B
7324/7-2
Novaya Zemlya
?
Kara Sea
Caledonides
B'
Baltic Shield
Kola Peninsula
Timan-Pechora Basin
Urals
A
A'
Unroofing of orogenic highlands
Deposition in high-accommodation basin
Triassic strata
Uralide Orogen
Pre-Mesozoic sedimentary rocks
B
B'
Exhumation and denudation of basin strata
Forebulge erosion
NZFTB
Uralide Orogen
Forebulge uplift
Recycled Late Triassic/ Early Jurassic strata

Table 1

Table 1. Locations of studied samples from the western Barents Shelf with estimated maximum burial depths.

Location	Formation	Age	Collected samples	Present Depth	Estimated uplift	Maximum burial depth
7324/7-2 Barents Sea (Hoop Fault Complex)	Fruholmen	Upper Triassic (Norian-Rhaetian)	19	737-780m MD	1800 m[1]	2537-2580m MD
	Stø	Early to Middle Jurassic (Toarcian to Bajocian)	11	710-735m MD	1800 m[1]	2510-2535m MD
Wilhelmøya (79.08144°N and 20.68276 °E, 79.06825°N and 20.72986°E)	Flatsalen	Upper Triassic (Norain)	8			
	Svenskøya	Late Triassic to Early Jurassic (Rhaetian to Toarcian)	3			

[1]Estimated uplift (Baig et al., 2016).